PERINTIS
Persatuan Saintis Muslim Malaysia

PERINTIS eJournal
Vol. 15, No. 2, Dec 2025, pp. 47-55
e-ISSN: 2232-0725, DOI: 10.5281/zenodo.18081296

Comparative Characterization Study of High-Q Optical Microbottle Resonators via Tapered Fibre Coupling at Neck and Maximum Curvature Regions

Sabrina Mohd Farid[1,2], Siti Nurul Fatihah Azahan[1,2], Muhammad Khudhori Mohd Yusof[1,2], Mohd Zamani Zulkifli[1,2]

[1]Department of Physics, Kulliyyah of Science, International Islamic University Malaysia, 25200, Kuantan, Pahang, Malaysia.
[2]IIUM Photonics and Quantum Centre, Kulliyyah of Science, International Islamic University Malaysia, 25200, Kuantan, Pahang, Malaysia.

Corresponding author: mzz@iium.edu.my

https://doi.org/10.5281/zenodo.18081296

Received 10 31, 2025
Revised 12 27, 2025
Accepted 12 29, 2025

ABSTRACT

Whispering gallery modes (WGM) such as microbottle resonators (MBR) is a miniature light confining photonics device and are a promising component in photonic systems such as sensors, lasers, and optical filters due to their efficient light confinement and compact geometry. However, the effect of coupling position on their optical performance remains insufficiently explored. This study investigates the fabrication and characterization of optical MBR using tapered fibre coupling at two regions which are the neck and the maximum curvature. The MBR was produced through controlled heating and surface-tension shaping of single-mode optical fibres, followed by precise light coupling via a tapered fibre. Experimental results show Q-factors of 12,597 at the neck and 16,989 at the maximum curvature, indicating stronger confinement and reduced scattering losses in the latter. These findings demonstrate the influence of coupling position on resonator performance and support the design of efficient microresonators for advanced photonic applications. Through the lens of Tawhidic epistemology, the ability of such microscopic structures to precisely confine and guide light reflects the immense power and wisdom of Allah.

Keywords: Whispering gallery modes (WGM); microbottle; tapered fibre coupling; coupling region; Q-factors.

1.0 INTRODUCTION

Optical microresonators are fundamental components in modern photonics, capable of trapping light through total internal reflection and enabling a wide range of high-performance applications. Among them, whispering gallery mode (WGM) resonators, such as microbottle resonators (MBR), exhibit remarkable optical confinement, making them highly attractive for sensing, lasing, nonlinear optics, and optical filtering applications [1]. In these structures, light circulates along the resonator surface with minimal radiation loss, resulting in extremely high quality (Q) factors and strong field enhancement [2]. WGM resonators have been realized in various geometries, including microtoroids, microdisks, microbottles, and microcylinders [3]–[6].

MBR differ from conventional microspheres and microtoroids by their elongated axial geometry, which supports both azimuthal and axial mode confinement. This unique structure enables enhanced axial mode control, tunable mode selection, and improved compatibility with fibre-based coupling schemes. However, due to the axial asymmetry of the microbottle geometry, the coupling position between the tapered optical fibre and the resonator surface plays a critical role in determining coupling efficiency, mode excitation, and spectral characteristics. The external coupling strength is governed by the spatial overlap between the evanescent field of the tapered fibre and the WGM field, which varies significantly along the axial direction of the microbottle.

Most previous studies on microbottle resonators have predominantly employed equatorial or maximum curvature coupling, as this region provides strong evanescent field overlap and facilitates efficient excitation of high-Q resonances. Consequently, experimental investigations have largely focused on coupling at or near the central region of the microbottle, while coupling at the neck region remains comparatively underexplored [7]. Nevertheless, theoretical and experimental studies have indicated that coupling depending on axial position can strongly influence the number of excited group mode families (GMFs), axial mode orders, and resonance linewidths due to axial mode cutoff and confinement effects inherent to the bottle geometry. In particular, coupling closer to the neck is expected to suppress certain axial standing-wave modes and modify the modal field distribution, offering an additional degree of freedom for spectral tailoring and mode selectivity.

Motivated by this research gap, the present study aims to fabricate high-Q optical microbottle resonators and systematically compare tapered fibre coupling at the neck and maximum curvature regions. By examining the transmission spectra, group mode family distributions, and Q-factors under both coupling configurations, this work seeks to clarify how axial coupling position governs light confinement and resonator performance. Such understanding is essential for optimizing microbottle-based devices for sensing and integrated photonic applications, where trade-offs between Q-factor, mode density, and field localization are critical.

In addition to its technical contribution, this study is framed within a Tawhidic epistemological perspective, wherein the precise and orderly behavior of light confined within microscopic resonant structures reflects the unity, balance, and perfection embedded in the laws of creation. This perspective highlights the harmony between scientific inquiry and an appreciation of divine order, reinforcing the broader significance of photonics research beyond technological advancement.

2.0 METHODOLOGY

The methodology comprises four main stages which are the fabrication of the microbottle resonators, fabrication of the tapered optical fiber, optical coupling and spectral characterization, and resonance analysis including quality-factor extraction and mode identification.

2.1 Microbottle Resonator Fabrication

The MBRs were fabricated using a core-to-core fusion splicing technique with an ACUTEQ ATS-80A fusion splicer, employing standard 125 μm single-mode optical fibre. The MBR geometry was formed through a controlled sequence of electric arc discharges and fibre gap adjustments to ensure repeatability and structural symmetry.

The fusion splicer was operated at a fixed arc power of 45%, with a discharge duration of 1600 ms and a cleave angle of 4°, under constant discharge intensity conditions. The inter-fibre gap was maintained consistently using the splicer's automatic core-to-core alignment function, ensuring reproducible fabrication of microbottle resonators with uniform geometry.

As summarized in Table 1, multiple electric arc discharges were initially applied to both fibre ends to locally soften and expand the glass, forming spherical-shaped tips driven by surface tension. Each arc discharge was applied with a pressing duration of approximately 2 s, repeated 15 times, to achieve uniform tip expansion. The inter-fibre gap was subsequently adjusted when necessary, using controlled alignment operations to compensate for axial separation resulting from glass melting and to bring the spherical tips into close proximity. Once sufficient proximity was achieved, the fibre ends were fused through two controlled alignment operations, forming a stable core-to-core joint. Additional electric arc discharges were then applied to the fused region with a pressing duration of approximately 2 s, repeated 25 to 30 times, to further heat and expand the fibre forming the microbottle shape as seen in Fig.1. During this stage, surface tension-driven reshaping of the molten region resulted in the formation of a smooth and symmetric microbottle structure.

Table 1: Optimized MBR fabrication parameters using an ACUTEQ ATS-80A fusion splicer.

Button	Frequency	Function
Arc	15	To allow the fusion splicer's electrode to heat up the fibre ends using electric discharge forming spherical-shaped tips.
Set	1	Pressing the set button once will reduce the gap between the spherical tips as both ends will be a distant after each electric discharge due to the melting tip.
Set	2	Pressing the set button 2 times will fused both fibre ends together.
Arc	25 to 30	To heat up the connected fused ends and allow them to further expand until the bottle-shaped is formed.

Figure 1: The fabricated MBR using a core-to-core fusion splicing technique with an ACUTEQ ATS-80A fusion splicer.

2.2 Tapered Optical Fibre Fabrication

The tapered optical fibre used for evanescent coupling was fabricated using the flame brushing technique as seen in Fig.2. The setup consisted of two Thorlabs 300 mm linear translation stages equipped with integrated controllers and stepper motors, which symmetrically pulled the fibre during tapering. The pulling speed was fixed at 0.4 mm/s, and the pulling distance was calibrated to achieve a uniform taper profile. A 125 μm single-mode fibre with an uncoated length of approximately 2 cm was used.

An oxybutane flame source served as the heat source during tapering. The burner motion was controlled by an additional linear translation stage connected to a microcontroller and powered by a 50 V, 4 A, single-output 175 W power supply, with a scanning speed of 0.0625 mm/s. During the tapering process, one end of the fibre was connected to a C-band erbium-doped fibre (EDF) amplified spontaneous emission (ASE) source, while the opposite end was connected to an OSA203 Optical Spectrum Analyzer (OSA) to continuously monitor the transmission spectrum and ensure adiabatic taper formation. The final taper waist diameter was approximately 1–1.5 μm, suitable for efficient evanescent coupling.

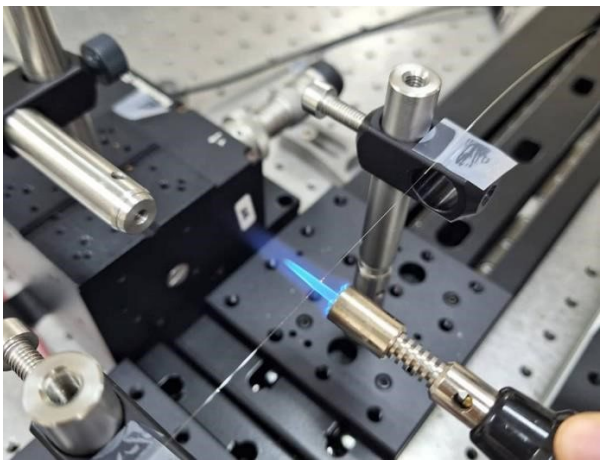

Figure 2: Tapered fibre fabrication process using the flame-brushing technique.

2.3 Optical Characterization and Coupling Configuration

Optical characterization of the fabricated microbottle resonators was performed using a tapered fibre coupling setup. Whispering gallery modes were excited via evanescent coupling by positioning the tapered fibre in close proximity to the microbottle surface. Two coupling configurations were investigated: neck region coupling and maximum curvature (central) region coupling, achieved by translating the tapered fibre along the axial direction of the microbottle, as illustrated in Fig. 3.

The transmitted optical signal was analysed using the OSA203 Optical Spectrum Analyzer, with sufficient wavelength resolution to resolve resonance features in the 1550 nm region. The total optical insertion loss of the system, including fibre taper loss and coupling loss, was estimated to be approximately 3 to 5 dB. Transmission spectra were recorded for both coupling positions to enable direct comparison of spectral characteristics.

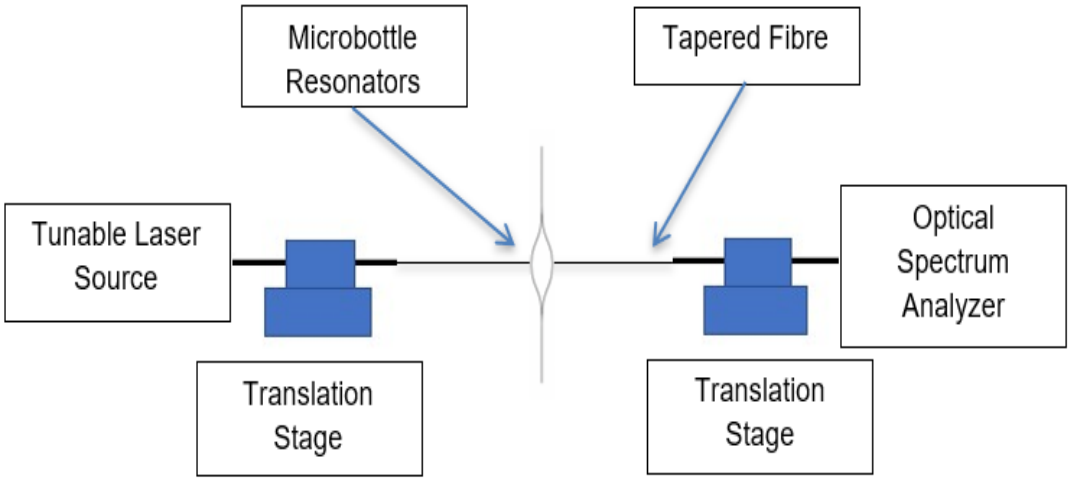

Figure 3. Experimental coupling configuration.

2.4 Data Analysis and Mode Identification

Resonance linewidths were extracted from the measured transmission spectra, and the quality factor (Q) was calculated using

$$Q = \frac{\lambda_0}{\Delta\lambda} \quad (1)$$

where $\lambda_0$is the resonant wavelength and $\Delta\lambda$ is the full width at half maximum (FWHM) of the resonance dip.

In a microbottle resonator, whispering gallery modes are characterized by three mode numbers: the azimuthal mode number (m) which corresponds to the number of wavelengths circulating around the resonator circumference, the radial mode number (p) which describes the field distribution across the radial direction of the resonator wall and the axial mode number (q), representing the standing-wave order along the bottle axis between the two neck regions. This mode classification follows the convention commonly adopted for microbottle resonators [7]. All measurements were conducted under ambient laboratory conditions at room temperature.

3.0 RESULTS AND DISCUSSION

The fabricated microbottles exhibited a maximum curvature diameter of 225 μm, axial length of 480 μm and neck diameter of 127 μm with smooth surfaces and well-defined curvature as seen in Fig.4.

Tapered fiber coupling at two distinct regions of the fabricated microbottle resonator, namely the maximum curvature (centre) and the neck region as seen in Fig.5. In both configurations, the evanescent field of the tapered fiber interacts with the resonator surface, enabling the excitation and circulation of whispering gallery modes (WGMs) along the microbottle. Beyond its physical significance, the controlled confinement and propagation of light within the resonator also symbolically reflect the concept of divine illumination, as expressed in Surah An-Nur (24:35): “Allah is the Light of the heavens and the earth.”

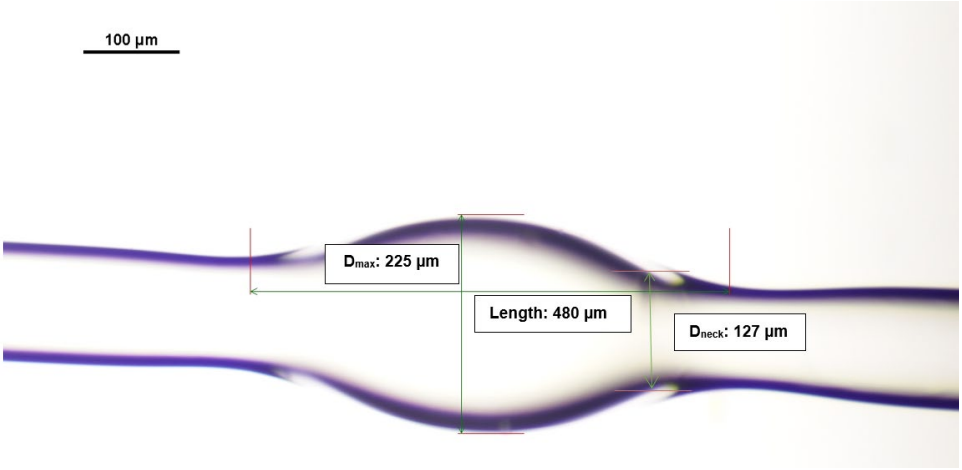

Figure 4: Geometrical characterization of the fabricated MBR the diameter of maximum curvature (D_{max}), diameter of neck region (D_{neck}) and overall axial length.

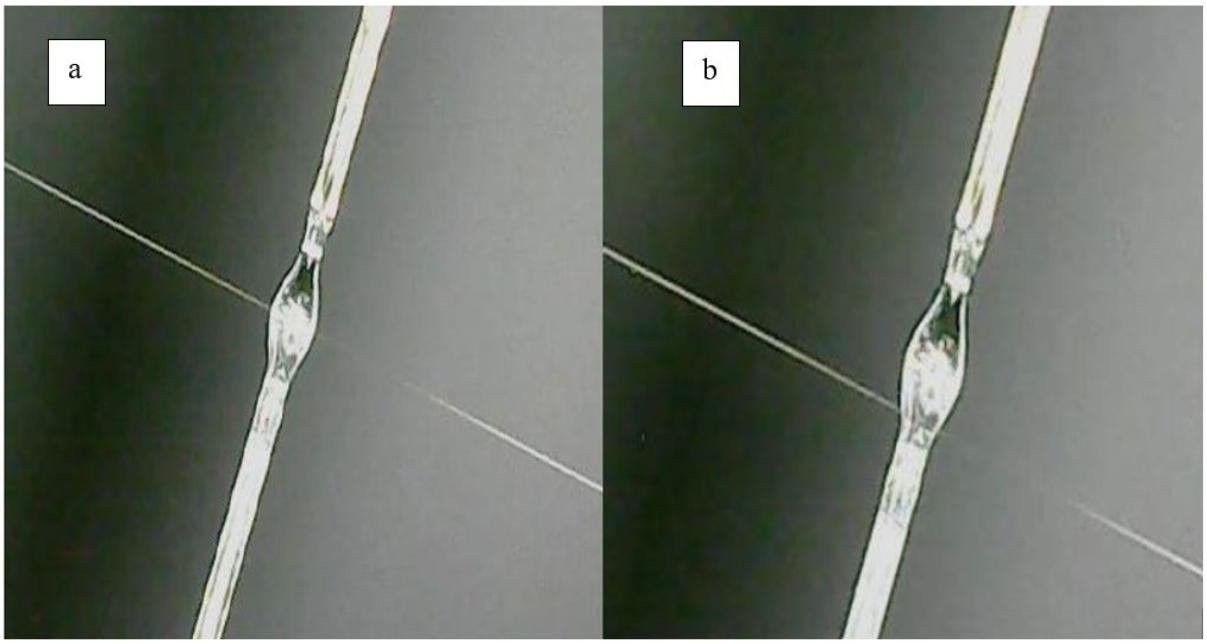

Figure 5: a) Coupling at centre of microbottle. b) Coupling at the neck of microbottle.

The transmission spectra presented in Fig. 6 confirm the formation of whispering gallery mode (WGM) resonances with distinct spectral characteristics for both coupling configurations. When coupling is performed at the maximum curvature (centre) region of the microbottle resonator (MBR), the transmission spectrum exhibits sharper and deeper resonance dips, whereas coupling at the neck region produces broader and shallower resonances. These spectral differeces indicate a strong dependence of resonator performance on the axial coupling position.

Quantitative analysis of the resonance linewidths reveals that coupling at the maximum curvature region yields a higher quality factor (Q-factor) compared to neck coupling. Specifically, centre coupling produces a resonance near 1550 nm with a narrow full width at half maximum (FWHM) of approximately 92 pm, corresponding to a Q-factor of 16,989. In contrast, neck-region coupling results in a slightly shifted resonance around 1550 nm with a broader FWHM of approximately 124 pm, yielding a lower Q-factor of 12,597 as seen in Table 2.

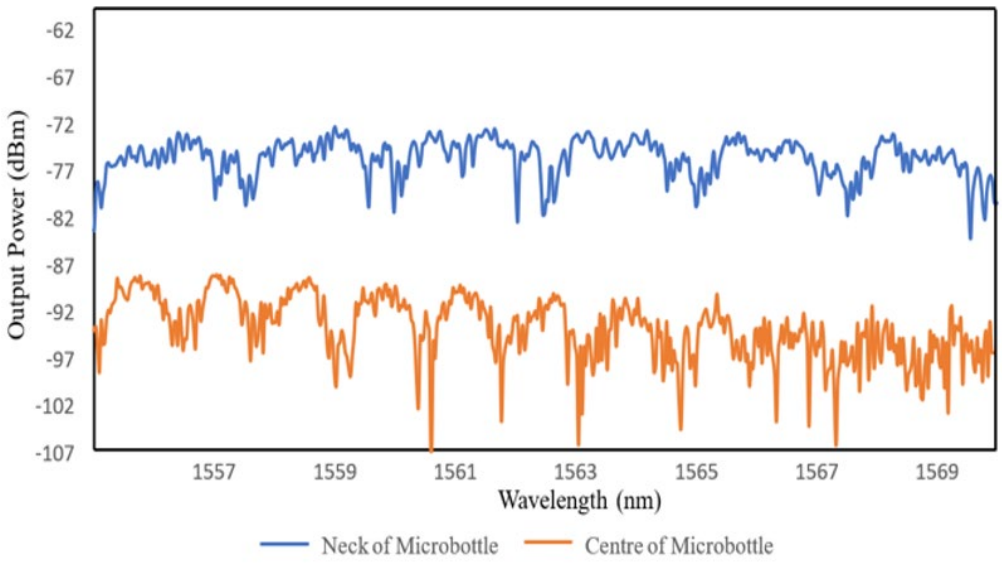

Figure 6: Coupling spectrum.

Table 2. Q-factors for different coupling positions.

Coupling Position	Resonant Wavelength (nm)	FWHM (pm)	Q-Factor
Neck Region	1562	124	12,597
Maximum Curvature	1563	92	16,989

In addition to the difference in Q-factor, Fig. 6 shows that a significantly larger number of WGM group mode families (GMFs) is excited when coupling at the centre of the MBR with 10 GMFs compared to coupling at the neck region with 6 GMFs. This behavior can be explained by coupling-position-dependent mode excitation in microbottle resonators. At the centre region, the larger local radius and weaker axial confinement enhance spatial overlap between the evanescent field of the tapered fibre and the resonator modes, enabling excitation of higher-order radial modes (p) as well as multiple axial standing-wave modes (q) [7–9]. Consequently, a denser mode spect 1557 1559 1561 1563 1565 1567 1569 Wavelength (nm)

Conversely, coupling near the neck region imposes stronger axial confinement due to the rapidly varying bottle radius and steeper curvature gradient. In this regime, several higher-order axial modes reach their cutoff condition and are no longer efficiently excited, thereby limiting the number of observable GMFs. This axial cutoff behavior has been theoretically and experimentally reported in microbottle resonators and leads to enhanced mode selectivity when coupling is performed near the neck region [8,9].

The higher Q-factor observed at the centre region can also be explained by the fundamental difference in light confinement mechanisms between the two coupling positions. According to the theory of whispering-gallery bottle microcavities acting as three-dimensional etalons, coupling near the neck excites axial bouncing-ball or Fabry–Perot–like modes, in which light propagates back and forth between the two neck regions of the microbottle [10,11]. This repeated axial reflection increases the probability of scattering and radiation losses, thereby reducing the overall Q-factor. In contrast, when coupling is performed at the centre region, light is predominantly confined near the maximum curvature and circulates azimuthally without significant axial bouncing between the necks. The suppression of axial back-and-forth propagation minimizes scattering loss and enhances energy storage within the resonator, resulting in a higher Q-factor [10,11].

Despite the lower Q-factor observed under neck coupling, this configuration remains of interest due to its distinct modal field distribution. The stronger axial confinement and modified evanescent field profile near the neck are expected to enhance interaction between the optical field and the surrounding environment. Such field localization effects are widely recognized as critical factors for refractive-index-based sensing using WGM resonators, including microbottle geometries [11-13]. While a direct sensitivity measurement is beyond the scope of the present study, the observed spectral behavior suggests that neck coupling provides a complementary operational regime to centre coupling, particularly for sensing-oriented designs.

Overall, these results demonstrate that the axial coupling position in a microbottle resonator governs both the quality factor and the modal landscape. Coupling at the centre region favours excitation of higher-order radial and axial modes, resulting in a larger number of GMFs and higher Q-factors suitable for applications such as narrow-line filtering, low-threshold lasing, and optical buffering. In contrast, coupling at the neck region suppresses higher-order modes, yielding fewer GMFs and enhanced mode selectivity, which may be advantageous for sensing applications. The comparative analysis highlights axial coupling control as a practical and powerful parameter for tailoring microbottle resonator performance.

4.0 CONCLUSION

This study successfully fabricated and characterized high Q optical microbottle resonators using tapered fibre coupling at different regions. The results revealed that coupling at the maximum curvature achieved a higher Q factor of 16,989 compared to 12597 at the neck region. The superior performance is attributed to stronger field confinement and reduced scattering losses, while the neck region remains valuable for high sensitivity sensing applications due to its stronger evanescent interaction with the surrounding medium. Beyond the technical findings, in the spirit of Tawhidic epistemology, this work offers a profound reflection on the harmony between light, matter, and divine design. Within a microsized strand of glass, light can circulate up to a million times, moving in perfect order along the curved boundary of the resonator. This astonishing phenomenon shows how precision and balance are woven into creation, allowing humans to harness light as sensors, filters, and instruments that improve life on Earth. It is a reminder that such perfection in nature is not by chance but a reflection of the divine wisdom of Allah, whose design and order are manifest even in the smallest structures of His creation.

ACKNOWLEDGEMENT

We would like to thank the Ministry of Higher Education of Malaysia for providing the grant of FRGS/1/2022/STG07/UIAM/02/1.

CONFLICT OF INTEREST

Competing interests: No relevant disclosures

REFERENCES

[1] Cai, L., Pan, J., Zhao, Y., Wang, J., & Xiao, S. (2020). Whispering gallery mode optical microresonators: structures and sensing applications. physica status solidi (a),217(6), 1900825. https://doi.org/10.1002/pssa.201900825

[2] Yu, D., Humar, M., Meserve, K., Bailey, R. C., Chormaic, S. N., & Vollmer, F. (2021). Whispering-gallery-mode sensors for biological and physical sensing. Nature reviews methods primers, 1(1), 83. https://doi.org/10.1038/s43586-021-00079-2

[3] F. Monifi, S. K. Özdemir, J. Friedlein and L. Yang, "Encapsulation of a Fibre Taper Coupled Microtoroid Resonator in a Polymer Matrix," in IEEE Photonics Technology Letters, vol. 25, no. 15, pp. 1458-1461, Aug.1, 2013, doi: 10.1109/LPT.2013.2266573. https://doi.org/10.1109/LPT.2013.2266573

[4] R. Saleem-Urothodi et al., "GaP WGM microdisks for second order nonlinear optics," 2024 24th International Conference on Transparent Optical Networks (ICTON), Bari, Italy, 2024, pp. 1-1. https://doi.org/10.1109/ICTON62926.2024.10647803
[5] A. Grimaldi, G. Testa, R. Bernini, S. Berneschi, F. Baldini and G. N. Conti, "A simple integration approach between self-assembled polymeric microbottle resonators and planar waveguide," 18th Italian National Conference on Photonic Technologies (Fotonica 2016), Rome, 2016, pp. 1-4, doi: 10.1049/cp.2016.0918. https://doi.org/10.1049/cp.2016.0918
[6] Y. Miao, Y. Peng, Y. Xiang, M. Li, Y. Lu and Y. Song, "Dynamic Fano Resonance in Thin Fibre Taper Coupled Cylindrical Microcavity," in IEEE Photonics Journal, vol. 8, no. 6, pp. 1-6, Dec. 2016, Art no. 4502806, doi: 10.1109/JPHOT.2016.2630316. https://doi.org/10.1109/JPHOT.2016.2630316
[7] Li, H. C., Liu, B., Wang, M. Y., Liu, J., He, X. D., Chan, H. P., ... & Wu, Q. (2021). Comparative study on sensing properties of fibre-coupled microbottle resonators with polymer materials. IEEE Sensors Journal, 21(23), 26681-26689. https://doi.org/10.1109/JSEN.2021.3122441
[8] Wang, M., Zhang, Y. N., Xiong, Y., Zhao, J., Lv, R., Han, B., & Zhao, Y. (2025). Design of a Vernier effect assisted optical fiber WGM microbottle for a highly sensitive temperature measurement. *Optics Letters*, *50*(8), 2482-2485. https://doi.org/10.1364/OL.546824
[9] Adnan Zain, H., Batumalay, M., Haris, H., Saad, I., Muhammad, A. R., Mustaffa, S. N., ... & Harun, S. W. (2023). Review of Microbottle Resonators for Sensing Applications. *Micromachines*, *14*(4), 734. https://doi.org/10.3390/mi14040734
[10] Sumetsky, M. (2004). Whispering-gallery-bottle microcavities: the three-dimensional etalon. *Optics letters*, *29*(1), 8-10. https://doi.org/10.1364/OL.29.000008
[11] Bianucci, P. (2016). Optical microbottle resonators for sensing. *Sensors*, *16*(11), 1841. https://doi.org/10.3390/s16111841
[12] F. Vollmer and S. Arnold, “Whispering-gallery-mode biosensing: label-free detection down to single molecules,” *Nature Methods*, 5, 591–596 (2008). https://doi.org/10.1038/nmeth.1221
[13] M. R. Foreman, J. D. Swaim, and F. Vollmer, “Whispering gallery mode sensors,” *Advances in Optics and Photonics*, 7, 168–240 (2015). https://doi.org/10.1364/AOP.7.000168